2014 IEEE International Conference on Fuzzy Systems (FUZZ-IEEE)
July 6-11, 2014, Beijing, China

Robust Adaptive Type-2 Fuzzy Logic Controller Design for a Flexible Air-breathing Hypersonic Vehicle

Fang. Yang, Jianqiang. Yi, Xiangmin. Tan, and Ruyi. Yuan

***Abstract*—A robust adaptive type-2 fuzzy logic controller is designed for the longitudinal dynamics of a flexible air-breathing hypersonic vehicle. The aircraft's pitch motion and flexible vibration are strongly coupled explicitly in the dynamic equations. The throttle setting is designed to control the velocity by dynamic inversion control method. The elevator deflection is designed to stabilize the pitch rate and flexible modes and in the end control the altitude in a stepwise manner by backstepping control method. The flexible modes are actively used in the control design in order to counteract both the tracking errors and the flexible vibrations. The virtual control signals in backstepping control as well as their derivatives are obtained by command filters whose magnitudes, bandwidths and rate limit constraints can be set. The transition processes of the velocity and altitude commands are also obtained by command filters. Uncertainties are estimated online by interval type-2 adaptive fuzzy logic system. The adaptive law of the fuzzy logic system is derived by Lyapunov synthesis approach. Simulation results demonstrate the effectiveness and robustness of the proposed controller and also validate type-2 fuzzy logic is more capable of handling uncertainties than type-1 fuzzy logic.**

NOMENCLATURE

V : velocity, ft/s	h : altitude, ft
γ : flight path angle, rad	α : angle of attack, rad
q : pitch rate, rad/s	L : lift, lb
D : drag, lb	T : thrust, lb
g : gravitational acceleration	M : pitching moment, lb·ft
m : mass, slug	I_y : moment of inertia, lb·ft^2
S : reference area, ft^2	c : mean aerodynamic chord, ft
$\bar{q}$: dynamic pressure, lb/ft^2	ρ : density of air, slugs/ft^3
ϕ_c : throttle setting instruction	ϕ : fuel equivalence ratio
δ_e : elevator deflection, rad	C_L : lift coefficient
C_D : drag coefficient	C_T : thrust coefficient

C_M : pitching moment coefficient

η_f, η_a : forebody and aftbody general elastic mode

ψ_f, ψ_a : forebody and aftbody coupling coefficient

ω_f, ω_a : forebody and aftbody natural frequency

ζ_f, ζ_a : forebody and aftbody damping ratio

Fang. Yang, Ruyi. Yuan, Jianqiang. Yi are all with the Institute of Automation, Chinese Academy of Sciences, Beijing 100190 China (corresponding author phone: +86-010-82544639; fax: 86-010-82544640; e-mail: ruyi.yuan@ ia.ac.cn).

This work was supported by National Natural Science Foundation of China under Grant 61203003, 61273149 and 60904006, Knowledge Innovation Program of the Chinese Academy of Sciences under Grant YYYJ-1122, and Innovation Method Fund of China under Grant 2012IM010200.

I. INTRODUCTION

HYPERSONIC vehicle has been widely researched since 1960s due to its high speed (at least 5 Mach), high thrust-to-weight ratio and reusability. It will dramatically reduce the flight time between continents and bring great development in civil and military applications. Although hypersonic vehicle has these advantages, its flight control law design is still highly challenging. Early research is mainly focused on a rocket-powered hypersonic vehicle called generic hypersonic flight vehicle (GHFV) [1]. GHFV is in winged-coned configuration which has complete ground test data. Its flight control law design neglected the flexible effects and viewed it as a rigid body. Xu designed an adaptive sliding mode controller on the high-order feedback linearized model and got good control effect and robustness under a certain degree of parametric uncertainty [2]. Some other representative control methods also can be seen in [3], [4].

The successful flight of scramjet-powered X-43 series promoted more research work on air-breathing hypersonic vehicle (AHV). AHV is in wave-rider configuration whose long-thin fuselage causes non-negligible structural vibration problem. Furthermore, due to AHV's special integrated engine-frame configuration, there exist tight and complex interactions between aerodynamics, structural dynamics and the propulsion system. Bolender developed a nonlinear model (called heave model) for the longitudinal dynamics of an AHV using Lagrange method [5], [6]. But heave model is too complex for control design. Three kinds of simplified models are derived from heave model as table Ⅰ shows. Rigid-body modes are nearly independent on flexible modes in model A. Relevant papers can be found in [7]. Model B gets the most widely used recently. It displays no coupling explicitly in dynamic equations but the flexible modes affect the aerodynamic and propulsive coefficients and therefore indirectly affect the rigid-body modes. Kuipers designed an adaptive linear quadratic controller based on the linearized rigid AHV model [8]. Lisa introduced the canard deflection as an additional control variable and designed the parameter adaptive law to guarantee the stability of the rigid-body dynamics and the flexible dynamics [9]. Parker also added the canard to eliminate the non-minimum phase character of the rigid-body dynamics and stabilized the flexible dynamics [10]. In this paper, we study model C which displays strong coupling in dynamic equations especially between the pitch motion and the flexible vibration but neglects the flexible effects on coefficients. Up to now, for model C, few papers have actively used flexible modes to design a control law. Model A and C adopt two-cantilever-beam assumptions and

978-1-4799-2072-3/14/$31.00 ©2014 IEEE

consider 2 first-order modal coordinates. Model B adopts one-free-beam assumption and considers 3 modal coordinates (including first, second and third-order).

TABLE I
3 KINDS OF SIMPLIFIED MODELS

Model	A	B	C
Equation coupling	×	×	√
Coefficient coupling	×	√	×
Beam assumption	cantilever	free	cantilever

√ means there exists equation or coefficient coupling whereas × means no coupling.

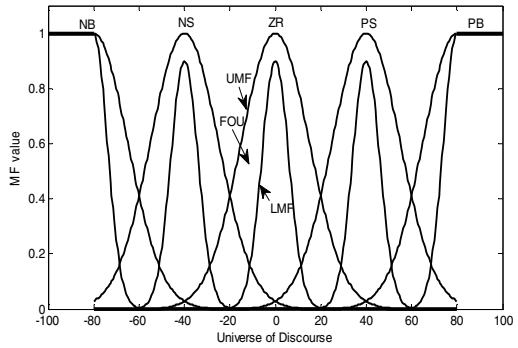

Fig. 1. Membership function example of IT2-FS

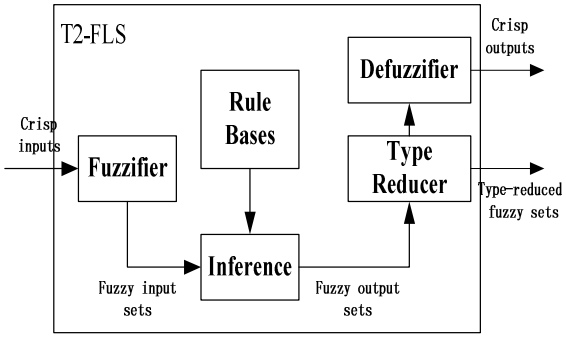

Fig. 2. The structure of T2-FLS.

Uncertainty is inevitable during control process. One feasible way is to estimate it online and actively counteract it. Type-2 fuzzy logic system (T2-FLS) is one such powerful estimator. Unlike traditional type-1 fuzzy set (T1-FS), the membership function (MF) of type-2 fuzzy set (T2-FS) is fuzzy itself which is so called primary MF. The MF of the primary MF is called secondary MF. An example of T2-FS's MF is shown in Fig.1. The region between the upper MF (UMF) and the lower MF (LMF) is called footprint of uncertainty (FOU). FOU adds an additional degree of freedom to the fuzzy set and makes it more capable of dealing with uncertain problem than T1-FS. The structure of T2-FLS is shown in Fig. 2. The type-2 fuzzy output set will not be used until it is type-reduced. The existence of type-reducer before defuzzifier is the most important difference from type-1 fuzzy logic system (T1-FLS). In order to reduce the computational cost, the interval T2-FS (IT2-FS) is used whose secondary MF grades are always 1 [11]. The widely used Karnik- Mendel algorithm (KMA) is chosen as the type reduction method [12]. Interval T2-FLS (IT2-FLS) has been used to estimate uncertain terms and shown its strong approximation capability [13]. Direct and indirect interval type-2 fuzzy logic controllers (IT2-FLCs) have been introduced in hypersonic control in my former papers [14]-[17].

This paper proposes a robust adaptive indirect interval type-2 fuzzy logic controller for a flexible air-breathing hypersonic vehicle. The flexible modes are actively used in the control law design. Uncertainties during control process are estimated online by IT2-FLS. The adaptive law is derived by Lyapunov synthesis approach. This paper is organized as follows: Section 2 describes the control problem and gives some preliminary knowledge. Section 3 designs the controller and the interval type-2 fuzzy logic system in detail. Section 4 derives the adaptive law and gives stability analysis. In section 5, simulations are conducted to validate the proposed controller. Conclusions are given in the final part.

II. PROBLEM STATEMENT AND PRELIMINARIES

The control objective is to design the throttle setting and elevator deflection to make the AHV track the velocity and altitude cruise command and meanwhile restrain the flexible vibration. In the following, we give some preliminary knowledge of the control problem.

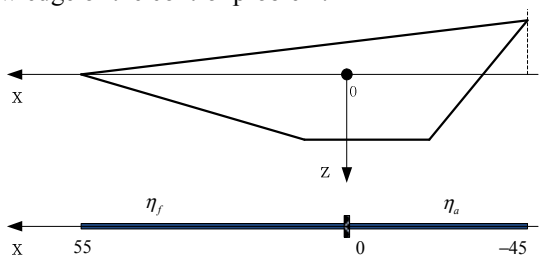

Fig. 3. Aircraft geometry and two cantilever beams coordinate system.

A. The Longitudinal Dynamics of the Flexible AHV

For a wave-rider configuration AHV, we assume that the fuselage is comprised of two cantilever beams which are clamped at the center-of-mass and only consider their first-order modal coordinates η_f and η_a. The coordinate system is chosen as Fig.3 shows. Then a strong coupled model (heave model) is derived [5], [6]. If we omit the relative small items in the heave model, we obtain the following simplified dynamic model:

$$\begin{cases} m\dot{U} + mqW + mg\sin\theta = F_x + T \\ m\dot{W} - mqU - mg\cos\theta = F_z \\ I_y\dot{q} - \psi_f\ddot{\eta}_f - \psi_a\ddot{\eta}_a = M \\ \ddot{\eta}_f - \dot{q}\psi_f + 2\zeta_f\omega_f\dot{\eta}_f + \omega_f^2\eta_f = N_f \\ \ddot{\eta}_a - \dot{q}\psi_a + 2\zeta_a\omega_a\dot{\eta}_a + \omega_a^2\eta_a = N_a \end{cases} \quad (1)$$

where U, W and F_x, F_z are velocity and forces along body axes x, z, N_f, N_a are general elastic forces of forebody and aftbody, $\psi_f = 363.5007$, $\psi_a = -328.8033$, $\omega_f = 16.0213$, $\omega_a = 19.5813$, $\zeta_f = \zeta_a = 0.02$. Transfering (1) from body coordinate system to wind coordinate system and after some

decoupling operation, we obtain (2) and (3):

$$\begin{cases} \dot{V} = \dfrac{T\cos\alpha - D}{m} - g\sin\gamma \\ \dot{\gamma} = \dfrac{L + T\sin\alpha}{mV} - \dfrac{g\cos\gamma}{V} \\ \dot{h} = V\sin\gamma \\ \dot{\alpha} = q - \dot{\gamma} \end{cases} \tag{2}$$

$$\begin{cases} \dot{q} = (M + \psi_f C_f + \psi_a C_a)/K \\ \ddot{\eta}_f = (\psi_f M + \psi_f \psi_a C_a + (I_y - \psi_a^2)C_f)/K \\ \ddot{\eta}_a = (\psi_a M + \psi_f \psi_a C_f + (I_y - \psi_f^2)C_a)/K \end{cases} \tag{3}$$

where $K = I_y - \psi_f^2 - \psi_a^2$, $C_f = N_f - 2\zeta_f\omega_f\dot{\eta}_f - \omega_f^2\eta_f$, $C_a = N_a - 2\zeta_a\omega_a\dot{\eta}_a - \omega_a^2\eta_a$. Equation (3) shows the strong coupling between pitch motion and flexible vibration. Coefficient details can be seen in [10].

B. Characteristic Roots Analysis

The dynamic equations (2) and (3) contain 9 state variables $\boldsymbol{x} = [V\ h\ \gamma\ \alpha\ q\ \eta_f\ \dot{\eta}_f\ \eta_a\ \dot{\eta}_a]^T$ (The variable in bold in this paper indicates that it is a vector). Linearize the model at the cruise point $V_0 = 7702.08$ ft/s, $h_0 = 85000$ ft, and then compute its characteristic roots as table Ⅱ shows.

TABLE II
CHARACTERISTIC ROOTS OF THE LINEARIZED MODEL

Mode	Characteristic roots
Altitude mode	0.0001203
Phugoid mode	-0.0008026±0.04031 i
Short period mode	1.685, -1.756
Forebody aeroelastic mode	-0.3589±17.28 i
Aftbody aeroelastic mode	-0.6787±25.00 i

From table Ⅱ we can see that the altitude mode is unstable and the phugoid mode is stable. The flexible vibration affects them little [18]. The short period mode contains one positive root and therefore is unstable, which indicates the motion of the angle of attack and the pitch rate is unstable. The forebody and aftbody aeroelastic modes are stable but their vibrational frequencies are close to the cantilevers' natural frequencies. The analysis shows the great difficulties in control design and also shows the control focuses.

C. Command Filter

Command filters are used to obtain the derivatives of the virtual control signals [19]. As Fig. 4 shows, command filter puts magnitude, bandwidth and rate limit on the source signal x_c^0 and outputs the revised signal x_c and its derivative $\dot{x}_c$. When the signal is within the limits, the transfer function from the input to the output is:

$$\frac{x_c(s)}{x_c^0(s)} = \frac{\omega_i^2}{s^2 + 2\zeta_i\omega_i s + \omega_i^2} \tag{4}$$

where ζ_i and ω_i are filter damping ratio and bandwidth. Command filter can also filter out high-frequency noise and get the transient process of the reference command signal.

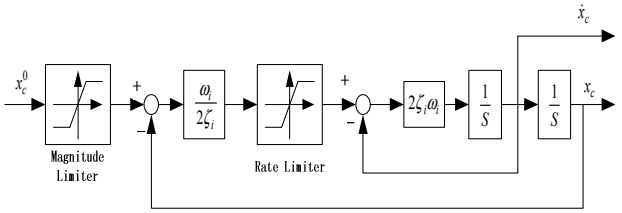

Fig. 4 Command filter with magnitude, bandwidth and rate limit constraints

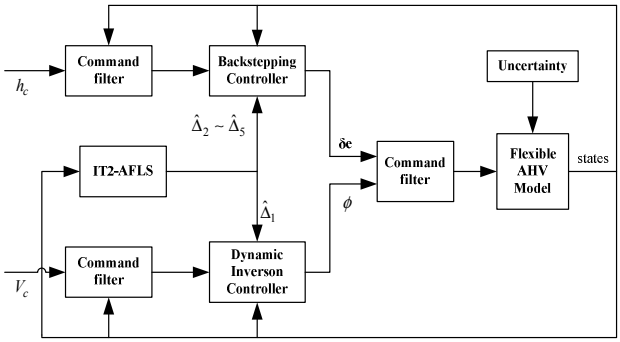

Fig. 5 The block diagram of the overall control scheme

III. CONTROL DESIGN

A. Overall Control Scheme

In order to simplify our control design, we divide the AHV dynamic equations into two subsystems: velocity subsystem and altitude subsystem. In velocity subsystem, the throttle setting ϕ is used to control velocity V to its reference signal V_c by dynamic inversion control method. In altitude subsystem, a backstepping controller is applied. The elevator deflection δ_e is used to stabilize pitch rate q as well as flexible modes η_f and η_a . Then q controls angle of attack α and flight path angle γ and finally guides altitude h to its reference signal h_c in a stepwise manner. The overall control scheme can be seen in Fig.5. Uncertainties during control process are estimated online by interval type-2 adaptive fuzzy logic system.

B. Velocity Subsystem Dynamic Inversion Controller Design

The error dynamics of the velocity is:

$$\begin{aligned} \dot{\tilde{V}} &= \dot{V} - \dot{V}_c = \frac{T\cos\alpha - D}{m} - g\sin\gamma - \dot{V}_c \\ &= \frac{T_\phi\cos\alpha}{m}\phi + \frac{T_x\cos\alpha - D}{m} - g\sin\gamma - \dot{V}_c \end{aligned} \tag{5}$$

Denote $f_1 = \dfrac{T_\phi\cos\alpha}{m}, g_1 = \dfrac{T_x\cos\alpha - D}{m} - g\sin\gamma$. Considering the modelling error, the computing error in aerodynamic coefficients, the measuring error of states' signals, the actuator delays and others (we see all the errors as general uncertainty), we introduce an additional item Δ_1^* to represent the general uncertainty . We obtain:

$$\dot{\tilde{V}} = f_1\phi + g_1 - \dot{V}_c - \Delta_1^* \tag{6}$$

The exact value of Δ_1^* is impossible to get. So we use a powerful interval type-2 adaptive fuzzy logic system (IT2-AFLS) to estimate it online and get $\hat{\Delta}_1$ instead. In order to stabilize the velocity tracking error, by dynamic inversion control, the control signal can be chosen as:

$$\phi_c = \frac{1}{f_1}[-g_1 + \dot{V}_c - k_1\tilde{V} + \hat{\Delta}_1] \tag{7}$$

And (6) can be rewritten as:

$$\dot{\tilde{V}} = -k_1\tilde{V} + (\hat{\Delta}_1 - \Delta_1^*) \tag{8}$$

C. Altitude Subsystem Backstepping Controller Design

1) Altitude Error Dynamics: The error dynamics of the altitude is:

$$\dot{\tilde{h}} = \dot{h} - \dot{h}_c = V\sin\gamma - \dot{h}_c \approx V\gamma - \dot{h}_c \tag{9}$$

Similar to the velocity subsystem, we introduce Δ_2^* to represent the general uncertainty in (8) and use $\hat{\Delta}_2$ to estimate it. Small change in γ will cause great change in h, so we choose γ as the virtual control signal. To stabilize the altitude tracking error, the flight path angle signal can be chosen as:

$$\gamma_c = \frac{\dot{h}_c - k_2\tilde{h} + \hat{\Delta}_2}{V} \tag{10}$$

And (9) can be rewritten as:

$$\dot{\tilde{h}} = -k_2\tilde{h} + (\hat{\Delta}_2 - \Delta_2^*) \tag{11}$$

2) Flight Path Angle Error Dynamics: The error dynamics of the flight path angle is:

$$\dot{\tilde{\gamma}} = \dot{\gamma} - \dot{\gamma}_c = \frac{\bar{q}SC_L^{\alpha}}{mV}\alpha + \frac{\bar{q}S(C_L^{\delta_e}\delta_e + C_L^0) + T\sin\alpha}{mV} - \frac{g\cos\gamma}{V} - \dot{\gamma}_c \tag{12}$$

In order to unify the subscript, we disuse f_2 and g_2 and denote $f_3 = \frac{\bar{q}SC_L^{\alpha}}{mV}, g_3 = \frac{\bar{q}S(C_L^{\delta_e}\delta_e + C_L^0) + T\sin\alpha}{mV} - \frac{g\cos\gamma}{V}$. Similarly we introduce Δ_3^* to represent the general uncertainty in (12) and use $\hat{\Delta}_3$ to estimate it. Because $C_L^{\alpha} \gg C_L^{\delta_e}$ and $\bar{q}SC_L^{\alpha}\alpha \gg T\sin\alpha$, γ is mainly driven by α. To stabilize the flight path angle tracking error, the virtual control signal can be chosen as:

$$\alpha_c = \frac{1}{f_3}[-g_3 + \dot{\gamma}_c - k_3\tilde{\gamma} + \hat{\Delta}_3] \tag{13}$$

And (12) can be rewritten as:

$$\dot{\tilde{\gamma}} = -k_3\tilde{\gamma} + (\hat{\Delta}_3 - \Delta_3^*) \tag{14}$$

3) Angle of Attack Error Dynamics: The error dynamics of the angle of attack is:

$$\dot{\tilde{\alpha}} = \dot{\alpha} - \dot{\alpha}_c = q - \frac{L + T\sin\alpha}{mV} + \frac{g\cos\gamma}{V} - \dot{\alpha}_c \tag{15}$$

Denote $g_4 = -\frac{L + T\sin\alpha}{mV} + \frac{g\cos\gamma}{V}$. The virtual control signal can be chosen as:

$$q_c = -g_4 + \dot{\alpha}_c - k_4\tilde{\alpha} + \hat{\Delta}_4 \tag{16}$$

And (15) can be rewritten as:

$$\dot{\tilde{\alpha}} = -k_4\tilde{\alpha} + (\hat{\Delta}_4 - \Delta_4^*) \tag{17}$$

3) Pitch Rate Error Dynamics: The error dynamics of the pitch rate is

$$\dot{\tilde{q}} = \dot{q} - \dot{q}_c = \frac{\bar{q}ScC_M^{\delta_e} + \psi_a N_a^{\delta_e}}{K}\delta_e - \dot{q}_c + \frac{\bar{q}ScC_M^x + z_T T + \psi_f C_f + \psi_a C_a^x}{K} \tag{18}$$

where $C_M^x = C_M(\alpha) = C_M - C_M^{\delta_e}\delta_e$, $N_a^x = N_a(\alpha) = N_a - N_a^{\delta_e}\delta_e$, $C_{ax} = N_a^x - 2\zeta_a\omega_a\dot{\eta}_a - \omega_a^2\eta_a$. Denote $f_5 = \frac{\bar{q}ScC_M^{\delta_e} + \psi_a N_a^{\delta_e}}{K}$, $g_5 = \frac{\bar{q}ScC_M^x + z_T T + \psi_f C_f + \psi_a C_{ax}}{K}$. The real control signal can be chosen as:

$$\delta_{ec} = \frac{1}{f_5}[-g_5 + f_q - k_5\tilde{q} + \dot{q}_c + \hat{\Delta}_5] \tag{19}$$

And (18) can be rewritten as:

$$\dot{\tilde{q}} = f_q + (\hat{\Delta}_5 - \Delta_5^*) \tag{20}$$

where f_q will be determined later in the stability analysis.

D. Type-2 Adaptive Fuzzy Logic System Design

As described in the former sections, uncertainty is inevitable in control design. One feasible solution is to actively estimate the uncertainty and use it to improve the controller robustness. Interval type-2 adaptive fuzzy logic system (IT2-AFLS) is one powerful tool to estimate large uncertainty. Here we use IT2-AFLS with pre-determined IT2 antecedent sets and adaptive T1 consequent sets to estimate $\hat{\Delta}_i$. The fuzzy rule bases consist of a collection of IF-THEN rules in the following form:

R_i^n : *If* $\tilde{x}_i$ *is* $\tilde{A}_i^n$ *and* $\dot{\tilde{x}}_i$ *is* $\tilde{B}_i^n$, *then* $\hat{\Delta}_i$ *is* C_i^n $n = 1,\ldots,M$

where x_i $(i = 1,...,5)$ represents the rigid body modes $(V, h, \gamma, \alpha, q)$, $\tilde{A}_i^n$, $\tilde{B}_i^n$ are IT2 fuzzy sets, C_i^n is T1 fuzzy set, M is the rule number. If $\tilde{A}_i^n$, $\tilde{B}_i^n$ each has 5 fuzzy sets, then $M = 5\times 5 = 25$. By using the singleton fuzzification, product inference and the center-of-sets (COS) type reducer [11], the type-reduced set is given by:

$$\Delta_{i\cos} = \int_{y_i^1}\cdots\int_{y_i^M}\int_{f_i^1}\cdots\int_{f_i^M}\frac{\prod_{n=1}^{M}\mu_{C_i^n}(y_i^n)\prod_{n=1}^{M}\mu_{F_i^n}(f_i^n)}{\sum_{n=1}^{M}f_i^n y_i^n \Big/ \sum_{n=1}^{M}f_i^n} \tag{21}$$

where y_i^n is the centroid of C_i^n and f_i^n is the firing value associated with the n^{th} rule. Here the centroid y_i^n is defined as the point which has the maximum membership value 1. As $\mu_{F_i^n}(f_i^n) = 1$, $\mu_{C_i^n}(y_i^n) = 1$,

$$\Delta_{i\cos}=\int_{y_i^1}\cdots\int_{y_i^M}\int_{f_i^1}\cdots\int_{f_i^M}\frac{1}{\frac{\sum_{n=1}^{M}f_i^n y_i^n}{\sum_{n=1}^{M}f_i^n}}=[\Delta_{il},\Delta_{ir}] \tag{22}$$

The type reduced set's bounds Δ_{il},Δ_{ir} are totally determined by $\sum_{n=1}^{M}f_i^n y_i^n\Big/\sum_{n=1}^{M}f_i^n$. Choose the following fuzzy basis function as:

$$\underline{\xi}_i^n=f_{il}^n\Big/\sum_{n=1}^{M}f_{il}^n,\ \overline{\xi}_i^n=f_{ir}^n\Big/\sum_{n=1}^{M}f_{ir}^n \tag{23}$$

where f_{il}^n,f_{ir}^n denote the firing values involved to compute Δ_{il},Δ_{ir} .There exist several computing methods referred as type reduction algorithms. Here we use the Karnik-Mendel algorithm (KMA) to obtain f_{il}^n,f_{ir}^n and all the algorithm details can be seen in [12].

The centroid y_i^n is viewed as an adaptive parameter and can be redenoted by new symbol θ_i^n . We get the bounds:

$$\Delta_{il}=\theta_i^n\underline{\xi}_i^n,\ \Delta_{ir}=\theta_i^n\overline{\xi}_i^n \tag{24}$$

Define $\underline{\boldsymbol{\xi}}_i=(\underline{\xi}_i^1,\underline{\xi}_i^2,...,\underline{\xi}_i^M)^T$, $\overline{\boldsymbol{\xi}}_i=(\overline{\xi}_i^1,\overline{\xi}_i^2,...,\overline{\xi}_i^M)^T$, $\boldsymbol{\xi}_i=(\underline{\boldsymbol{\xi}}_i+\overline{\boldsymbol{\xi}}_i)\big/2$, $\boldsymbol{\theta}_i=(\theta_i^1,\theta_i^2,...,\theta_i^M)^T$. By center-average defuzzification, the output of the fuzzy logic system is:

$$\hat{\Delta}_i=(\Delta_{il}+\Delta_{ir})/2=\boldsymbol{\theta}_i^T\boldsymbol{\xi}_i \tag{25}$$

IV. Adaptive Law and Stability Analysis

Denote $\tilde{\boldsymbol{x}}=[\tilde{V}\ \tilde{h}\ \tilde{\gamma}\ \tilde{\alpha}\ \tilde{q}]^T$, $\tilde{\boldsymbol{\theta}}_i=\hat{\boldsymbol{\theta}}_i-\boldsymbol{\theta}_i^*$, $\tilde{\Delta}_i=\hat{\Delta}_i-\Delta_i^*=\tilde{\boldsymbol{\theta}}_i^T\boldsymbol{\xi}_i$, where $\boldsymbol{\theta}_i^*$ is the truth value. $k_i(i=1,...,4)$ are positive constants, $p_i(i=1,...,7)$ are positive weights, $\tau_i(i=1,...,5)$ are positive learning rates. $\tilde{\eta}_f=\eta_f-\eta_f^*$, $\tilde{\eta}_a=\eta_a-\eta_a^*$, where η_f^*,η_a^* are the trim values. Then the rigid body modes error dynamics can be written as:

$$\begin{cases}\dot{\tilde{x}}_i=-k_i\tilde{x}_i+\tilde{\Delta}_i, i=1,...,4\\ \dot{\tilde{x}}_5=f_q+\tilde{\Delta}_5\end{cases} \tag{26}$$

Consider the following Lyapunov function candidate:

$$V_L=\sum_{i=1}^{5}\frac{p_i}{2}\tilde{x}_i^2+\sum_{i=1}^{5}\frac{1}{2\tau_i}\tilde{\boldsymbol{\theta}}_i^T\tilde{\boldsymbol{\theta}}_i+\frac{1}{2}(p_6\omega_f^2\tilde{\eta}_f^2+p_7\omega_a^2\tilde{\eta}_a^2+p_6\dot{\eta}_f^2+p_7\dot{\eta}_a^2) \tag{27}$$

The time derivative of V_L is:

$$\dot{V}_L=\sum_{i=1}^{5}p_i\tilde{x}_i\dot{\tilde{x}}_i+\sum_{i=1}^{5}\frac{1}{\tau_i}\tilde{\boldsymbol{\theta}}_i^T\dot{\hat{\boldsymbol{\theta}}}_i+p_6\omega_f^2\tilde{\eta}_f\dot{\eta}_f+p_7\omega_a^2\tilde{\eta}_a\dot{\eta}_a+p_6\dot{\eta}_f\ddot{\eta}_f+p_7\dot{\eta}_a\ddot{\eta}_a \tag{28}$$

On the other hand, from the fourth and fifth equations of (1), we get:

$$\begin{cases}\ddot{\eta}_f=\psi_f\dot{q}+N_f-2\zeta_f\omega_f\dot{\eta}_f-\omega_f^2\eta_f\\ \ddot{\eta}_a=\psi_f\dot{q}+N_a-2\zeta_a\omega_a\dot{\eta}_a-\omega_a^2\eta_a\end{cases} \tag{29}$$

where

$$\dot{q}=\dot{\tilde{q}}+\dot{q}_c=f_q+\tilde{\Delta}_5+\dot{q}_c \tag{30}$$

Substituting (26), (29), (30) to (28), we get:

$$\begin{aligned}\dot{V}_L=&-\sum_{i=1}^{4}p_ik_i\tilde{x}_i^2-2p_6\zeta_f\omega_f\dot{\eta}_f^2-2p_7\zeta_a\omega_a\dot{\eta}_a^2\\&+\sum_{i=1}^{4}\tilde{\boldsymbol{\theta}}_i^T(\frac{1}{\tau_i}\dot{\hat{\boldsymbol{\theta}}}_i+p_i\tilde{x}_i\boldsymbol{\xi}_i)\\&+\tilde{\boldsymbol{\theta}}_5^T[\frac{1}{\tau_5}\dot{\hat{\boldsymbol{\theta}}}_5+(p_6\psi_f\dot{\eta}_f+p_7\psi_a\dot{\eta}_a+p_5\tilde{q})\boldsymbol{\xi}_5]\\&+[f_q(p_6\psi_f\dot{\eta}_f+p_7\psi_a\dot{\eta}_a+p_5\tilde{q})+\dot{q}_c(p_6\psi_f\dot{\eta}_f+p_7\psi_a\dot{\eta}_a)\\&+p_6(N_f-\omega_f^2\eta_f^*)\dot{\eta}_f+p_7(N_a-\omega_a^2\eta_a^*)\dot{\eta}_a]\end{aligned} \tag{31}$$

So, by Lyapunov synthesis approach, the adaptive law of the interval type-2 adaptive fuzzy logic system can be:

$$\begin{cases}\dot{\hat{\boldsymbol{\theta}}}_i=\boldsymbol{Proj}(-p_i\tau_i\tilde{x}_i\boldsymbol{\xi}_i),\ i=1,2,3,4\\ \dot{\hat{\boldsymbol{\theta}}}_5=\boldsymbol{Proj}(-\tau_5(p_6\psi_f\dot{\eta}_f+p_7\psi_a\dot{\eta}_a+p_5\tilde{q})\boldsymbol{\xi}_5)\end{cases} \tag{32}$$

where *Proj*(•) is the projection operator which guarantees all parameters are in their allowed compact sets. Denote $C_q=p_6\psi_f\dot{\eta}_f+p_7\psi_a\dot{\eta}_a+p_5\tilde{q}$, $C_{q_c}=\dot{q}_c(p_6\psi_f\dot{\eta}_f+p_7\psi_a\dot{\eta}_a)$, $C_\eta=p_6(N_f-\omega_f^2\eta_f^*)\dot{\eta}_f+p_7(N_a-\omega_a^2\eta_a^*)\dot{\eta}_a$. If C_q is far away from zero, f_q can be chosen as (33) to cancel the last bracket of (31).

$$f_q=-\frac{\dot{q}_cC_{q_c}+C_\eta}{C_q} \tag{33}$$

When C_q is near zero, (33) is infinite and there exist two cases. In Case one, the system is already stable and all $\dot{\eta}_f,\dot{\eta}_a,\tilde{q}$ and the last bracket of (31) are near zero. In Case two, the sum of the three terms in C_q happens to be near zero, but at least one of $\dot{\eta}_f,\dot{\eta}_a,\tilde{q}$ is not zero (so the system does not come stable). In Case two, we let $f_q=0$ and soon the system moves to a condition that C_q is far away from zero in which (33) works. $f_q=0$ also makes sense in case one, because all C_q,C_{q_c},C_η are near zero and the last bracket of (31) can be canceled. Choose $\varepsilon=0.001$ as the threshold, so

$$f_q=\begin{cases}-\dfrac{\dot{q}_cC_{q_c}+C_\eta}{C_q}, & |C_q|>\varepsilon\\ 0, & |C_q|\le\varepsilon\end{cases} \tag{34}$$

By (32) and (34), (31) becomes:

$$\dot{V}_L=-\sum_{i=1}^{4}p_ik_i\tilde{x}_i^2-2p_6\zeta_f\omega_f\dot{\eta}_f^2-2p_7\zeta_a\omega_a\dot{\eta}_a^2<0 \tag{35}$$

So the closed loop system is stable by Lyapunov synthesis approach.

V. Simulation Resultes

At the pseudo trimmed condition: $V_0=7702.08$ ft/s, $h_0=85000$ ft, $\gamma_0=0$ rad, $\alpha_0=0.02453$ rad, $q_0=0$ rad/s, $\eta_{f0}=0.8983$, $\eta_{a0}=0.7400$, $\dot{\eta}_{f0}=\dot{\eta}_{a0}=0$, $\delta_{t0}=0.2505$, $\delta_{e0}=0.2092$. The reference command signals are chosen as

$\Delta V = 500$ ft/s and $\Delta h = 1000$ ft. The Learning rates $\tau_i = 0.01,\ i = 1,...,5$. The weights $p_1 = 1$, $p_2 = 1$, $p_3 = 1$, $p_4 = 1$, $p_5 = 5$, $p_6 = 0.1$, $p_7 = 0.1$. The coefficients $k_1 = 10$, $k_2 = 0.1$, $k_3 = 0.5$, $k_4 = 2$. Frequencies of the command filters are $\omega_v = 0.1$, $\omega_h = 0.1$, $\omega_\gamma = \omega_\alpha = \omega_q = 40$, $\omega_e = 50$, $\omega_t = 50$ and all damping ratios ζ_i are chosen as 1. Choose Gaussian function which has the same centre but different variances as the primary MF of IT2-FS. UMF has large variance and LMF has small variance. The initial values of the adaptive parameter vector $\boldsymbol{\theta}_i$ are randomly chosen. The parametric uncertainties are chosen as:

$$\begin{cases} m = m_0(1+U_f+U_g*GWN) \\ I_y = I_{y0}(1+U_f+U_g*GWN) \\ \rho = \rho_0(1+U_f+U_g*GWN) \\ S = S_0(1+U_f+U_g*GWN) \\ c = c_0(1+U_f+U_g*GWN) \end{cases} \tag{36}$$

where $m_0, I_{y0}, \rho_0, S_0, c_0$ are in nominal parameter values, U_f is the fixed parameter uncertainty and U_g is the strength of the Gaussian white noise (GWN) whose power is 0.002. Simulations are conducted for IT2-AFLC and T1-AFLC in two circumstances: A) without uncertainty and B) with uncertainty.

A. Simulation Results without Parametric Uncertainty

At the pseudo trim condition, if we input the constant control signals without any control strategy, the AHV's states will diverge after a few seconds, as Fig. 6 and Fig. 7 show. We can see that the velocity and altitude drop and the flexible modes vibrate sharply. It validates the former characteristic roots analysis.

The simulation results will be given during the conference.

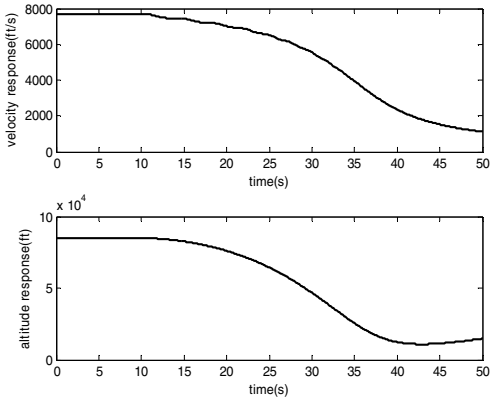

Fig. 6 Velocity and altitude response without control strategy

Set $U_f = U_g = 0$, then all parameters are in nominal values and there exists no uncertainty.

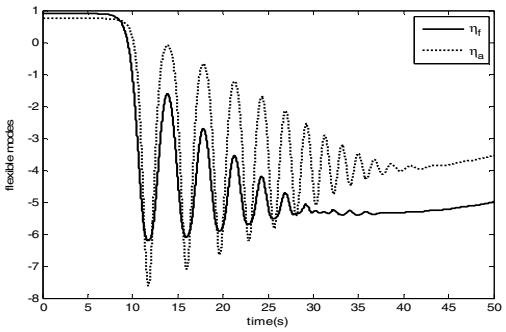

Fig. 7 Flexible modes response without control strategy

B. Simulation Results with Large Parametric Uncertainty

Set $U_f = 0.2$ and $U_g = 0.8$. Then all parameters are corrupted by fixed uncertainty and noise.

VI. Conclusion

The appearance of the flexible modes in the dynamic equations makes it very difficult to design a robust controller. This paper actively used the flexible modes and designed a robust adaptive controller to stabilize the tracking errors and the structural vibrations. An observer will be designed to estimate them online. Other kind of controllers will also be considered to obtain better robustness.

References

[1] J. D. Shaughnessy, S. Z. Pinckney, J. D. MacMinn, C. I. Cruz, and M. Kelley, "Hypersonic vehicle simulation model: winged-cone configuration," NASA Technical Memorandum, NASA-TM-102610, Nov. 1990.

[2] H. Xu, M. D. Mirmirani, and P. A. Ioannou, "Adaptive sliding mode control design for a hypersonic flight vehicle," *Journal of Guidance, Control, and Dynamics*, vol. 27, no. 5, 2004.

[3] Q. Wang and R. E. Stengel, "Robust nonlinear control of a hypersonic aircraft," *Journal of Guidance, Control, and Dynamics*, vol. 23, no. 4, 2000.

[4] B. Meng and H. Wu, "Adaptive control based on characteristic model for a hypersonic flight vehicle," in *Proc. 26th Chinese Control Conference*, Zhangjiajie, Hunan, China, pp. 720–724, 2007.

[5] M. A. Bolender and D. B. Doman, "A non-linear model for the longitudinal dynamics of a hypersonic air-breathing vehicle," *AIAA Guidance, Navigation, and Control Conference and Exhibit*, San Francisco, USA, Aug. 2005.

[6] M. A. Bolender and D. B. Doman, "Nonlinear longitudinal dynamical model of an air-breathing hypersonic vehicle," *Journal of Spacecraft and Rocket*, vol. 44, no. 2, 2007.

[7] C. Sun, Y. Huang, C. Qian, and L. Wang, "On modeling and control of a flexible air-breathing hypersonic vehicle based on LPV method," *Frontiers of Electrical and Electronic Engineering*, vol. 7, iss. 1, pp. 56–68, 2012.

[8] M. Kuipers, M. Mirmirani, P. Ioannou, and Y. Huo, "Adaptive control of an aeroelastic airbreathing hypersonic cruise vehicle," *AIAA Guidance, Navigation and Control Conference and Exhibit*, Hilton Head, USA, Aug. 2007.

[9] L. Fiorentini, A. Serrani, M. A. Bolender, and D. B. Doman, "Nonlinear robust adaptive control of flexible air-breathing hypersonic vehicles," *Journal of Guidance, Control, and Dynamics*, vol. 32, no. 2, 2009.

[10] J. T. Parker, A. Serrani, S. Yurkovich, M. A. Bolender, and D. B. Doman, "Control-oriented modelling of an air-breathing hypersonic vehicle," *Journal of Guidance, Control, and Dynamics*, vol. 30, no. 3, pp. 856–869, 2007.

[11] Q. Liang and J. M. Mendel, "Interval type-2 fuzzy logic systems: theory and design," *IEEE Trans on Fuzzy Systems*, vol. 8, no. 5, pp. 535–550, 2000.
[12] N. N. Karnik and J. M. Mendel, "Centroid of a type-2 fuzzy set," *Information Sciences,* vol. 132, iss. 1-4, pp. 195–220, 2001.
[13] T. Lin, H. Liu, and M. Kuo, "Direct adaptive interval type-2 fuzzy control of multivariable nonlinear systems," *Engineering Applications of Artificial Intelligence*, vol. 22, no. 3, pp. 420-430, 2009.
[14] F. Yang, J. Yi, X. Tan, and R. Yuan, "Direct adaptive type-2 fuzzy neural network control for a generic hypersonic flight vehicle," *Soft Computing*, vol. 17, iss. 11, pp. 2053-2064, 2013.
[15] F. Yang, X. Tan, and J. Yi, "A type-2 adaptive fuzzy logic controller for a generic hypersonic flight vehicle," *ICIC Express Letters*, vol.7, no.5, pp. 1583-1588, 2013.
[16] F. Yang, R. Yuan, J. Yi, G. Fan, and X. Tan, "Direct adaptive type-2 fuzzy logic control of a generic hypersonic flight vehicle," in *Proc. 4th International Conference on Intelligent Control and Information Processing*, pp. 581-586, 2013.
[17] F. Yang, R. Yuan, J. Yi, G. Fan, and X. Tan, "Backstepping based type-2 adaptive fuzzy control for a generic hypersonic flight vehicle," in *Proc. Chinese Intelligent Automation Conference, Lecture Notes in Electrical Engineering*, vol. 254, pp. 169-177, 2013.
[18] H. Li, *Hypersonic Flight Vehicle Guidance and Control Technology*. Beijing: China Astronautic Publishing House, 2012, ch. 7.
[19] J. Farrell, M. Sharma, and M. Polycarpou, "Backstepping-based flight control with adaptive function approximation," *Journal of Guidance, Control, and Dynamics*, vol. 28, no. 6, pp. 1089-1102, 2005.